PNAS
www.pnas.org

Supplementary Information for

Simple binding of protein kinase A, prior to phosphorylation, allows CFTR anion channels to be opened by nucleotides

Csaba Mihályi, Iordan Iordanov, Beáta Töröcsik, and László Csanády

Corresponding author: László Csanády
Email: csanady.laszlo@med.semmelweis-univ.hu

This PDF file includes:

Figures S1 to S6
SI References

www.pnas.org/cgi/doi/10.1073/pnas.2007910117

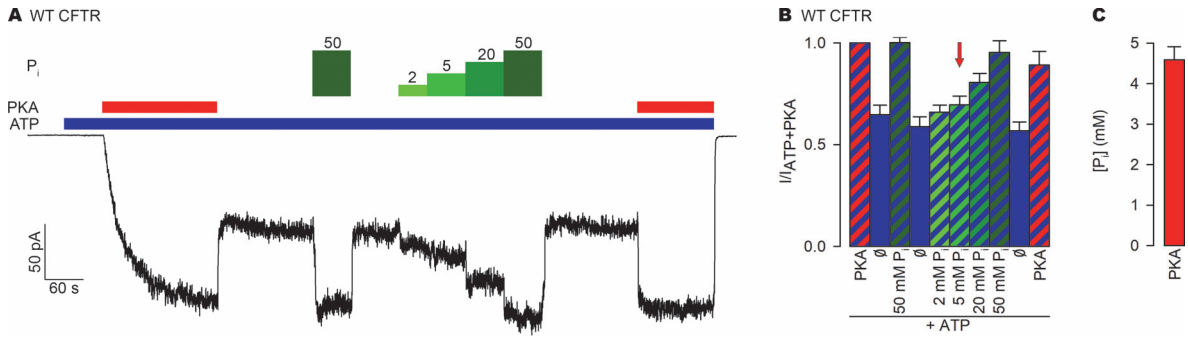

Fig. S1. Reversible stimulation by PKA, of phosphorylated WT CFTR channels gating in ATP, is not explained by contaminating P_i. A, Macroscopic WT CFTR current in an inside-out patch exposed to 2 mM ATP (*blue bar*), 300 nM PKA (*red bars*), and various concentrations of P_i (*green bars* with numbers (in mM)). **B,** Steady-state current amplitudes (mean±SEM (n=5)), normalized to that observed during the first exposure to ATP+PKA, for the ten segments of the experimental protocol shown in A, as indicated below the bars. Red arrow marks approximate [P_i], ~5 mM, present in the 300 nM PKA solution. **C,** Measured (see Materials and Methods) [P_i] in our bath solution supplemented with 300 nM PKA (mean±SEM (n=3)).

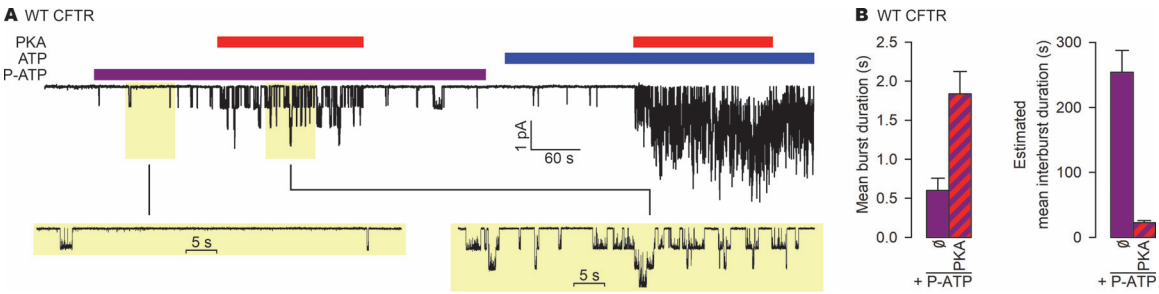

Figure S2. Gating kinetics of unphosphorylated WT CFTR channels in P-ATP, in the absence and presence of PKA. A, Microscopic current elicited by sequential exposures of a patch, containing at least 8 WT CFTR channels, to 300 nM PKA (*red bars*) first in the presence of 10 μM P-ATP (*purple bar*) and then in the presence of 2 mM ATP (*blue bar*). *Insets* show 1-minute current segments of unphosphorylated channels in P-ATP (*left*) and P-ATP+PKA (*right*) at an expanded time scale. **B,** *Left,* Steady-state mean burst durations (τ_b; mean±SEM (n=11, 13)) in the absence and presence of PKA, obtained through maximum-likelihood multi-channel dwell-time analysis (1). Note, that τ_b can be reliably estimated in patches containing multiple channels, even if the number of channels in the patch is unknown. *Right*, estimated steady-state mean interburst durations (τ_{ib}), calculated as $\tau_{ib} \sim \tau_b * ((1-P_o)/P_o)$. P_o values for the two conditions were estimated by multiplying the fractional macroscopic current obtained under identical conditions in macropatches (Fig. 3B, *leftmost two bars*) with the P_o (~0.35) of fully phosphorylated channels gating in PKA+ATP (2).

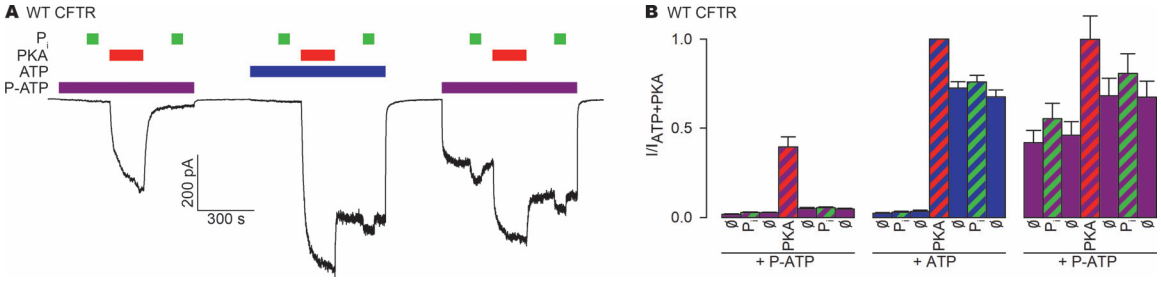

Fig. S3. Reversible stimulation by PKA, of unphosphorylated or phosphorylated WT CFTR channels gating in P-ATP, is not explained by contaminating P_i. A, Inside-out macropatch current elicited by applications of either 300 nM PKA (*red bars*) or 5 mM P_i (*green bars*) to WT CFTR channels gating in the presence of either 2 mM ATP (*blue bar*) or 10 μM P-ATP (*purple bars*). **B,** Steady-state current amplitudes (mean±SEM (n=6-9)), normalized to that observed during the first exposure to ATP+PKA, for the twenty-one segments of the experimental protocol shown in **A**, as indicated below the bars.

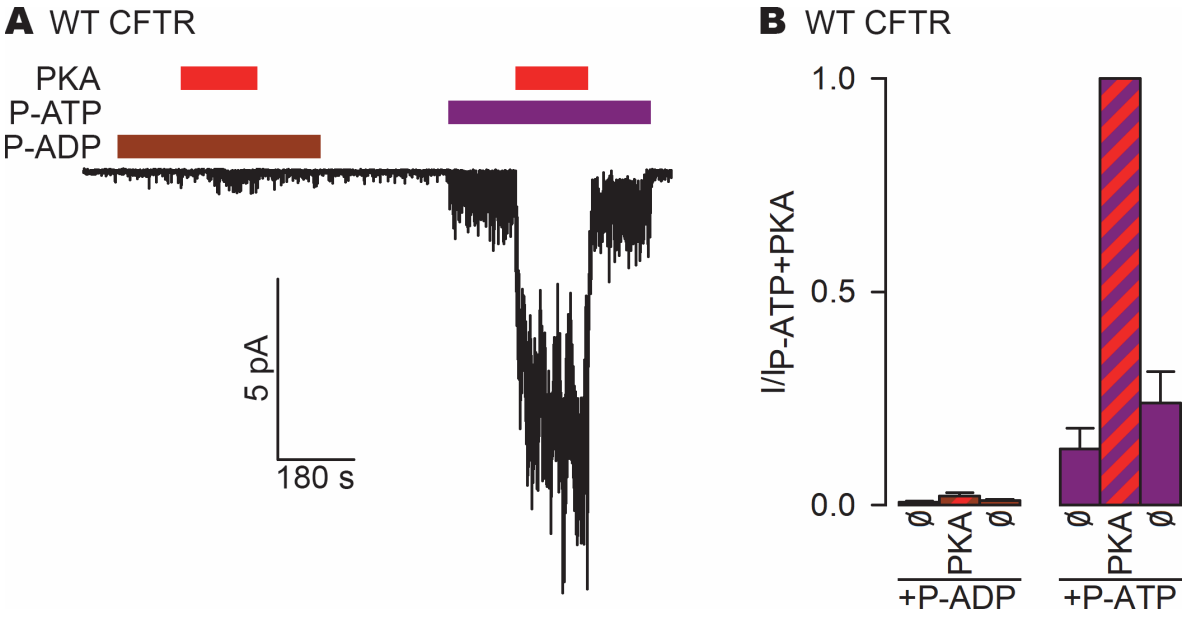

Fig. S4. Reversible stimulation by PKA, of unphosphorylated WT CFTR channels gating in P-ATP, is not explained by the P-ADP contaminant of the P-ATP stock. A, Inside-out current elicited by sequential exposures of a macropatch, containing unphosphorylated WT CFTR channels, to 300 nM PKA (*red bars*) first in the presence of 10 μM P-ADP (*brown bar*) and then in the presence of 10 μM P-ATP (*purple bar*). Note lack of effect of P-ADP on channel gating relative to background (i.e., infrequent spontaneous openings), as well as lack of effect of PKA under such conditions. As a control, the second part of the protocol (in P-ATP) recapitulates the findings shown in Fig. 3A-B (*left*). **B,** Steady-state current amplitudes (mean±SEM (n=4)), normalized to that observed during the second exposure to PKA (in P-ATP), for the six segments of the experimental protocol shown in **A,** as indicated below the bars. (Note different ordinate scaling, relative to Fig. 3B.)

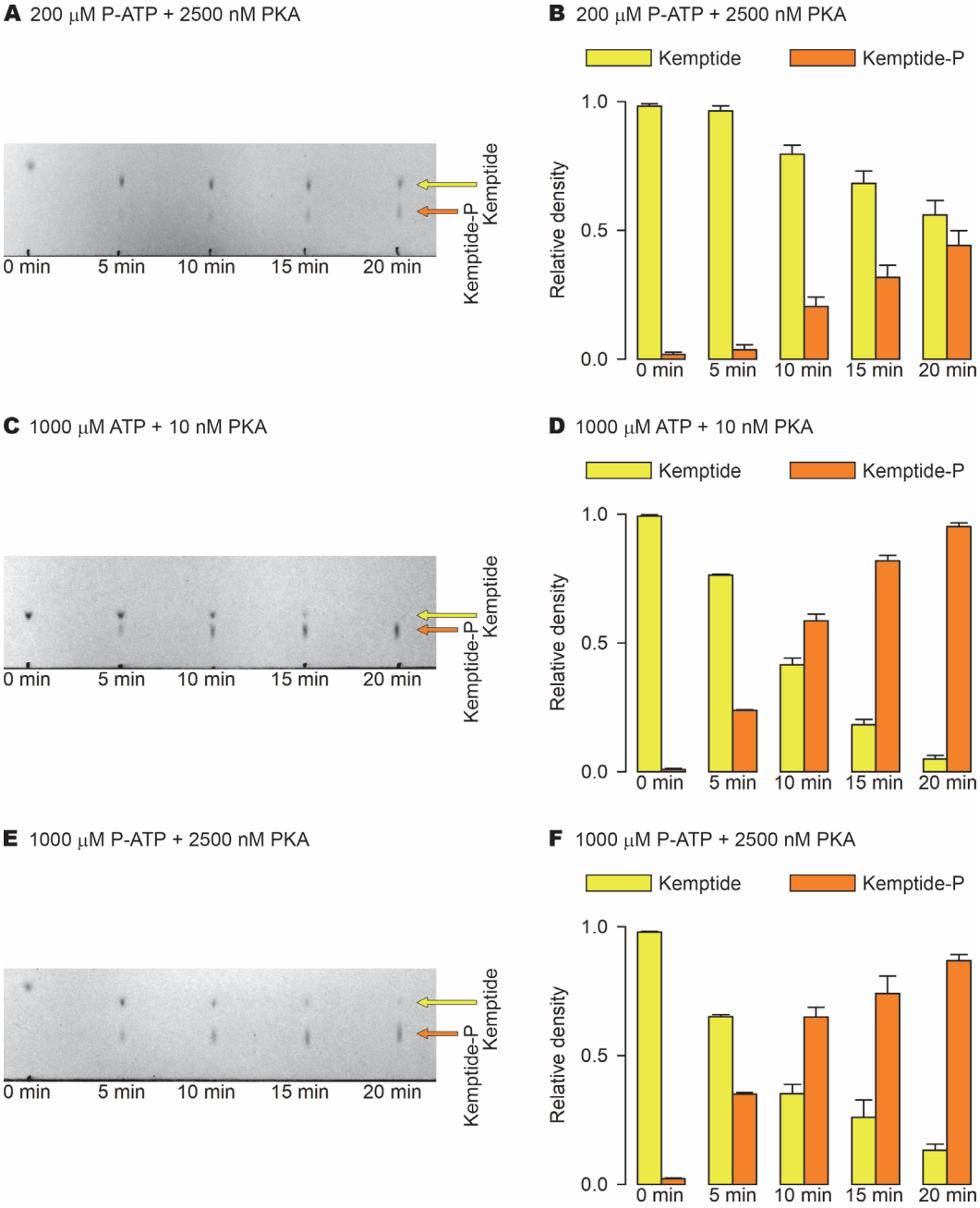

Fig. S5. Estimation of rates of phosphorylation by PKA using ATP or P-ATP for phosphotransfer. A, C, E, Kinetics of phosphorylation of TAMRA-kemptide (20 μM) by (**A**) 2500 nM PKA in the presence of 200 μM P-ATP, (**C**) 10 nM PKA in the presence of 1000 μM ATP, (**E**) 2500 nM PKA in the presence of 1000 μM P-ATP, visualized by TLC. *Yellow* and *orange arrows* mark the positions of the spots corresponding to the dephospho- and phosphopeptide, respectively. **B, D, F,** Densitometric analysis of the TLC sheets in (**A, C, E**). Relative densities (see Methods) of the dephospho- (*yellow bars*) and phospho-kemptide *(orange bars*) spots, plotted as a function of incubation time in PKA+ATP (**D**) or PKA+P-ATP (**B, F**). Bars plot mean±SEM (n=3).

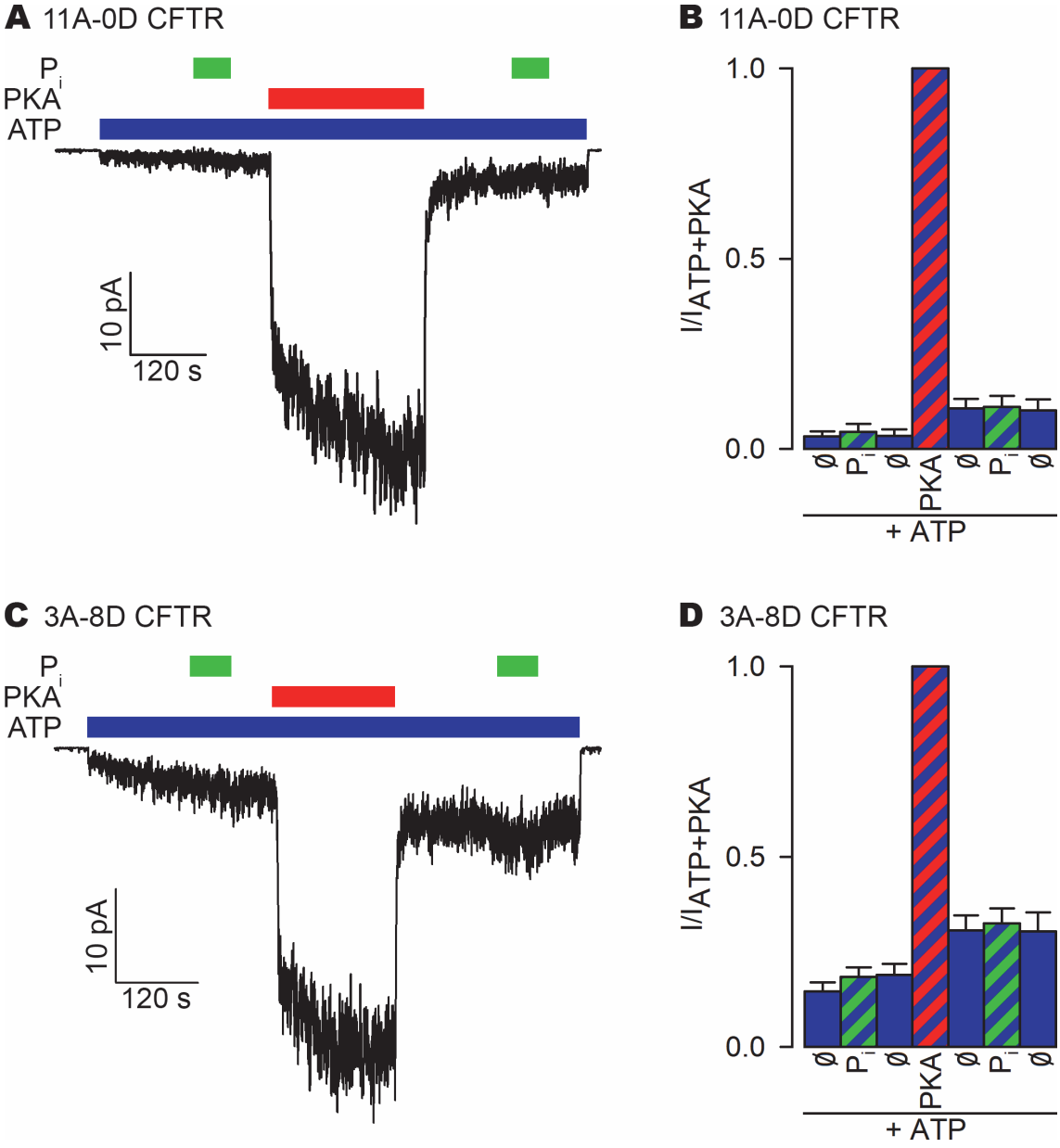

Fig. S6. Reversible stimulation by PKA, of mutant CFTR channels lacking phosphorylatable serines, is not explained by contaminating P_i. A, C, Macroscopic 11A-0D (**A**) and 3A-8D (**C**) CFTR currents in inside-out patches exposed to either 300 nM PKA (*red bar*) or 5 mM P_i (*green bars*) in the presence of 2 mM ATP (*blue bar*). **B, D,** Steady-state current amplitudes (mean±SEM (n=4-8)), normalized to that observed during the exposure to ATP+PKA, for the seven segments of the experimental protocol shown in **A, C,** as indicated below the bars.

SI References

1. L. Csanády, Rapid kinetic analysis of multichannel records by a simultaneous fit to all dwell-time histograms. *Biophys. J.* **78**, 785-799 (2000).

2. L. Csanády, P. Vergani, D.C. Gadsby, Strict coupling between CFTR's catalytic cycle and gating of its Cl− ion pore revealed by distributions of open channel burst durations. *Proc. Natl. Acad. Sci. U. S. A* **107**, 1241-1246 (2010).